01 Jun 1993

Temporal Effects in Multiphoton Ionization of Lithium

J. Greg Story
Missouri University of Science and Technology, story@mst.edu

Thomas F. Gallagher

Recommended Citation

J. G. Story and T. F. Gallagher, "Temporal Effects in Multiphoton Ionization of Lithium," *Physical Review A*, vol. 47, no. 6, pp. 5037-5040, American Physical Society (APS), Jun 1993.
The definitive version is available at https://doi.org/10.1103/PhysRevA.47.5037

Temporal effects in multiphoton ionization of lithium

J. G. Story and T. F. Gallagher
Department of Physics, University of Virginia, Charlottesville, Virginia 22901
(Received 13 November 1992)

The temporal effects of multiphoton ionization are investigated using a two-color method which determines both the time and intensity at which the process occurs. We show that the total ionization efficiency depends strongly on the time at which an atom makes a transition to an excited state during an intense laser pulse. This result clearly shows that the ac-Stark-shifted bound-state resonances not only enhance the cross section for photoionization, but that the excited bound states provide temporary storage states for the atomic population during the photoionization process.

PACS number(s): 32.80.Rm, 32.80.Wr

In recent years, with the advent of short-pulse, high-intensity lasers, multiphoton ionization of atoms in intense fields has received a great deal of study [1–8]. It has been shown that the atomic structure of the atom plays an important role in multiphoton ionization. Specifically, excited atomic states are brought into intermediate resonance with the ground state by the ac Stark shifts produced by the high laser intensities [1], and for multiphoton ionization of noble gases, much of the observed ionization is due to multiphoton resonance enhancement. Each bound excited state is shifted into resonance with the ground state at a single intensity, and only at these intensities can the excitation occur [3]. The intermediate resonances can provide more than just resonant enhancement of the photoionization process. The excited bound states can also act as storage states for the atomic population. In this case, the photoionization process can be seen as a two-step process in which an atom first makes a transition to an excited state and later is photoionized [9]. In this two-step process, the amount of ionization of the excited state should depend strongly on when during the laser pulse the atom makes a transition to the excited state. If the transition occurs early in the pulse, then there will be a relatively higher probability of photoionization than if the atom makes the transition later in the pulse. Recent work that has investigated the population left in these excited states after the laser pulse provides evidence of this two-step process [9]. Other recent work has suggested that the contribution of the two-step process is minimal, by showing that the multiphoton ionization of argon by short pulses occurs predominantly as a single-step process [10]. In this paper, we present an experimental investigation of this two-step process that clearly shows the dependence of the photoionization signal on the time during the laser pulse when the atom makes a transition to the excited state. We have used a two-laser technique that allowed us to temporally resolve the excitation of the atoms within the pulse of the ionizing laser. This resolution was not possible in the single-laser experiments of Refs. [9] and [10]. Both the observations presented here and the previous ones [9] are compatible with a Floquet description [11,12].

As seen in the energy-level diagram of Fig. 1, a 5-ps dye laser (561 nm) is tuned so that one photon from the dye laser and one photon of the 1.064-μm radiation is near the frequency of the 2s-to-3s transition of Li. From the 3s state, two photons of the 1.064-μm radiation can photoionize the atom. In the presence of the intense

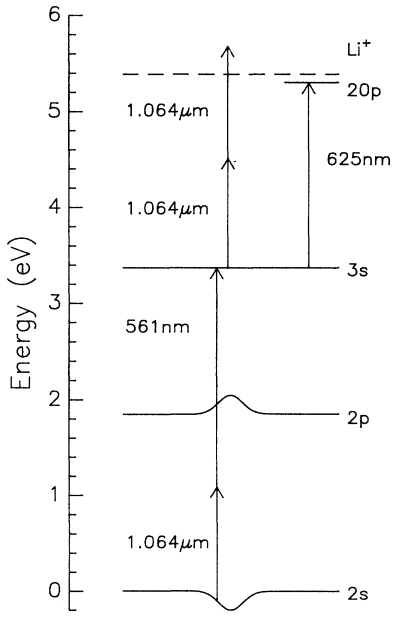

FIG. 1. Relevant eigenstates of Li are shown with the photons involved in the transition to the 3s state and to the continuum. One photon from the 5-ps dye laser and one photon from the 110-ps, 1.064-μm Nd:YAG laser excite the 2s-to-3s transition. From the 3s state, two 1.064-μm photons can ionize the atom. The timing of the dye laser determines when during the 1.064-μm pulse the atoms are excited, and the tuning of the dye laser determines the intensity of the 1.064-μm laser during excitation. After the ps pulses, a 5-ns, 625-nm pulse excites the atoms left in the 3s state to the 20p state, where they can be field ionized.

1.064-μm radiation, the energy level of the $2s$ ground state of Li is shifted downward with respect to the $3s$ state. The dye laser is sufficiently low in intensity that it produces a negligible shift of the atomic states and negligible photoionization of the $3s$ state. The shift of the ground state is mainly due to the relatively near-resonant interaction with the $2p$ state, which is also shown in the diagram. The dye-laser frequency can be tuned so that only those atoms with a specific shift can be excited resonantly to the $3s$ state. In this way, only atoms in the presence of a specific 1.064-μm intensity can be excited. By adjusting the relative delay between the 5-ps dye-laser pulse and the 110-ps 1.064-μm pulse, it is possible to choose the time during the 1.064-μm pulse when the atoms are excited. In other words, we can choose both the time and intensity at which the atoms are excited [13]. The two-photon ionization of the atom from the $3s$ state is a function of the exposure to the 1.064-μm pulse subsequent to excitation to the $3s$ state. Ten nanoseconds after the 1.064-μm pulse, the 625-nm, 5-ns laser is used to drive the $3s$-to-$20p$ transition, and atoms in the $20p$ state are then field ionized. In this way, the residual population of the $3s$ state is observed.

In the experiment, we use a Coherent Antares 76-s continuous-wave (cw) mode-locked Nd:YAG laser, which produces 110-ps pulses of 1.064-μm radiation. The light is frequency doubled to produce 532-nm light, which is used to pump a Coherent 700 mode-locked cw dye laser, which produces 5-ps pulses near 561 nm. The residual 1.064-μm light from the mode-locked Nd:YAG laser is amplified by a Continuum regenerative amplifier, which runs at 15 Hz and produces 110-ps pulses of approximately 40 mJ energy. This light is frequency doubled and used to pump a Continuum three-stage dye amplifier, which amplifies the dye laser to produce 5-ps pulses of approximately 0.2 mJ energy. The bandwidths of both the 1.064-μm and 532-nm pulses were transform limited. Also used in the experiment is a Quanta-Ray DCR1 Nd:YAG laser to pump a dye laser, which produces 5-ns, 1-mJ pulses at 625 nm, with a bandwidth of 1 cm^{-1}.

The ps dye-laser beam travels through a variable delay line consisting of a right-angle prism mounted on a translation stage. The ps dye-laser beam is then combined with the residual 1.064-μm beam from the regenerative amplifier using a dichroic dye-laser mirror, which reflects the 561-nm dye-laser light and passes the 1.064-μm light. The two beams, which have Gaussian spatial profiles, pass through a lens system that collimates the 561-nm beam to a beam waist of approximately 1 mm full width at half maximum (FWHM) and tightly focuses the 1.064-μm beam to a beam waist of approximately 30 μm FWHM in the interaction region. The 1.064-μm beam has a pulse energy of 2.8 mJ, giving a peak intensity of approximately 2×10^{12} W/cm^2. The 561-nm dye laser has a pulse energy of 0.2 mJ, giving an intensity of 4×10^{9} W/cm^2. The 625-nm, 5-ns dye-laser beam is collimated to a beam waist of approximately 1 mm and counterpropagates with the two ps beams, overlapping with them in the interaction region. In the interaction region inside a vacuum chamber, which operates at 10^{-7} torr, the three laser beams are crossed at right angle by an effusive beam of lithium atoms.

Ionization data were acquired using a pair of capacitor plates spaced by approximately 1 cm, located above and below the interaction region. The top plate, with a screen mesh in the center to allow the passage of ions, was grounded. The bottom plate was held at a small positive voltage (10 V) to push the ions produced by photoionization up into a micro-channel-plate detector above the interaction region. After the laser pulses, the bottom-plate voltage was increased to 8000 V to field ionize the $20p$ state. The high voltage was ramped on with a rise time of 1 μs, which is short compared to the $20d$ lifetime of 3.7 μs [14,15]. The ions produced by field ionization were also detected by the microchannel plates, which produced a second signal separated in time. Both signals were averaged using a box-car integrator and stored in a 7090A Hewlett Packard chart recorder.

Data were taken by setting the frequency of the ps dye-laser beam to a specific detuning of the combined Nd:YAG and dye-laser frequencies from the $2s$-$3s$ frequency and scanning the relative delay between the dye-laser pulse and 1.064-μm pulse. Scans were taken for detunings ranging from 0 to 90 cm^{-1}. Figure 2(a) shows the field-ionization signal as a function of the relative timing for a range of detunings. The data of Fig. 2(a) represent the residual $3s$ population following excitation by the ps pulses. This population is excited to the $20p$ state from which it is field ionized. The dashed line is a Gaussian distribution with the temporal parameter of the 1.064-μm laser pulse. Note that, with the exception of the lowest shifts, virtually no signal is seen outside the bounds of the Gaussian distribution. The signal outside of the Gaussian bounds for the lowest shifts is due to a slight tail of the laser pulse. Outside the boundary, there is insufficient intensity to produce the shift necessary for resonant excitation to the $3s$ state. As the detuning is increased, the temporal region becomes narrower and the boundary moves in towards the peak of the 1.064-μm pulse. For sufficiently large detunings (90 cm^{-1}), there is insufficient intensity even at the peak of the pulse to produce the required shift, and no population transfer is observed. For smaller detunings (60–80 cm^{-1}), very little residual population of the $3s$ state is seen. At these detunings, nearly all atoms that are excited to the $3s$ state are photoionized.

Figure 2(b) shows the photoionization of the $3s$ state. Again there is no signal seen outside the Gaussian boundary. The data for the larger detunings (70–90 cm^{-1}) are symmetric about the peak of the pulse. For these detunings, and the corresponding intensities, the photoionization of the $3s$ state is saturated. Virtually all atoms that are excited at these intensities are photoionized, regardless of when they make the transition to the $3s$ state. For smaller detunings, the signal is peaked near the front edge of the Gaussian distribution. For these smaller detunings and corresponding lower intensities, atoms that make the transition to the $3s$ state early in the 1.064-μm pulse are much more likely to be photoionized because they are exposed to a much larger flux of 1.064-μm photons after their excitation. For the 10-cm^{-1} shift, there is virtually no photoionization if the atoms are excited after

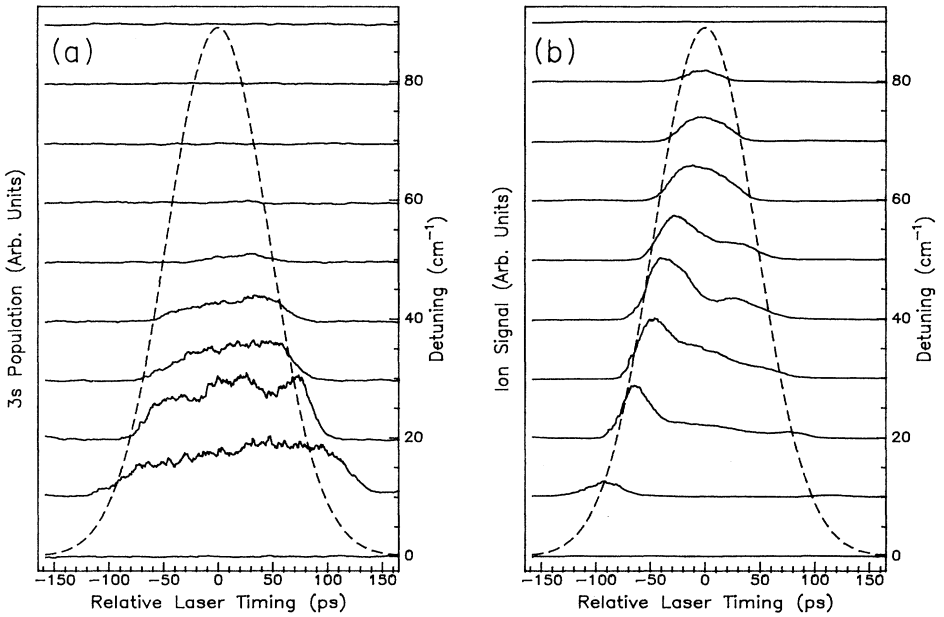

FIG. 2. (a) Residual $3s$ population after the ps laser pulses as a function of relative timing of the dye laser to the 1.064-μm pulse. For negative times, the dye-laser pulse comes before the peak of the 1.064-μm pulse. Data are shown for detunings of 0 to 90 cm^{-1} from the Li $2s$-$3s$ resonance. The dashed line shows the temporal profile of the 1.064-μm pulse. Outside the boundary of the pulse, there is little excitation of the $3s$ state, while inside the boundary, the excitation is relatively constant. (b) The photoionization signal vs the relative timing. Again there is virtually no signal outside the bounds of the 1.064-μm pulse. For the lower detunings, corresponding to lower intensity, only atoms excited on the rising edge of the 1.064-μm pulse are photoionized. For the higher detunings, the ionization is saturated for all times and the signal again is symmetric about the 1.064-μm pulse.

the leading edge of the pulse, even though Fig. 2(a) shows a large population transfer to the $3s$ for this detuning. For small detunings, the $3s$ state evidently acts as a storage state for population during the evolution of the 1.064-μm pulse. The fact that no ionization is seen for small detunings late in the 1.064-μm pulse, though the $3s$ state is populated, ensures that all photoionization seen is due to the 1.064-μm laser. Photoionization of the $3s$ state due to the 532-nm laser would depend only on the $3s$-state population and not on the relative timing or the detuning. For these reasons, we can rule out the possibility of photoionization by the 532-nm laser.

Figure 3 shows the ionization efficiency of the $3s$ state for a detuning of 50 cm^{-1}. This curve results from dividing the photoionization signal of Fig. 2(b) by the total signal of Fig. 2(a) and Fig. 2(b). It is important to note that the intensity at which the atoms are excited to the $3s$ state is the same for all atoms regardless of when they are excited. Only the temporal evolution of the pulse after the excitation is responsible for the changing ionization probability. The change of the $3s$ population per unit time is given by

$$dp = -p\sigma\Phi^2 dt \ , \tag{1}$$

where σ is the two-photon photoionization cross section and Φ is the photon flux, given by

$$\Phi = \Phi_{\max} \exp(-t^2/\tau^2) \ , \tag{2}$$

where τ is the characteristic time constant of the 1.064-μm pulse. Equation (1) can be integrated, assuming p is initially 1, to give

$$\int_1^p \frac{dp}{p} = \ln(p) = \int_{t_0}^{\infty} -\sigma\Phi^2 dt = -\sigma\Phi_{\max}^2 \operatorname{erfc}(\sqrt{2}t_0/\tau) \ . \tag{3}$$

In terms of the photon flux at time t_0, given by

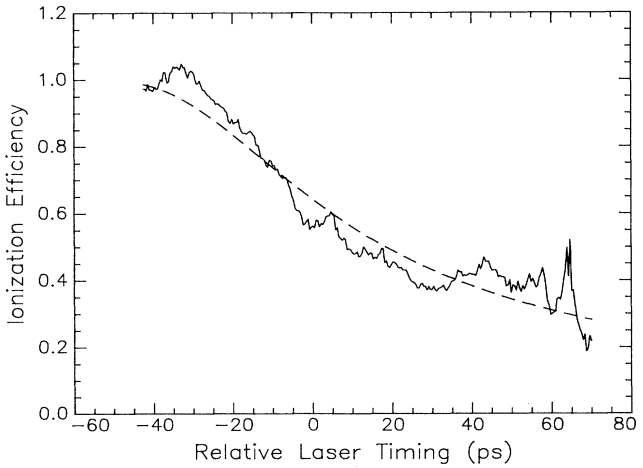

FIG. 3. Photoionization efficiency of the $3s$ state is shown for a detuning of 50 cm^{-1}. An efficiency of 1 corresponds to total ionization. This graph was obtained by dividing the photoionization signal of Fig. 2(b) by the total signal of Fig. 2(a) and Fig. 2(b). Also shown is a fit of the data using Eq. (1).

$$\Phi_0=\Phi_{\max}\exp(-t_0^2/\tau^2)\ , \tag{4}$$

the final population of the $3s$ state is

$$p=\exp[-\sigma\Phi_0^2\exp(2t_0^2/\tau^2)\mathrm{erfc}(\sqrt{2}t_0/\tau)]\ . \tag{5}$$

The probability of ionization of the $3s$ state after excitation at time t_0 is given by

$$P_{\mathrm{ion}}=1-p=1-\exp[-\sigma\Phi_0^2\exp(2t_0^2/\tau^2)\mathrm{erfc}(\sqrt{2}t_0/\tau)]\ . \tag{6}$$

This function is plotted with the data in Fig. 3, which represents the ionization efficiency of the $3s$ state independent of the initial population. The value of $\sigma\Phi_0^2$ was chosen to obtain the best fit to the data. This function shows saturation for decreasing values of t_0 and drops rapidly for increasing values. An atom excited to the $3s$ state very early in the pulse will see a much larger peak intensity than an atom that is excited at or beyond the peak of the laser pulse.

For the normal one-color short-pulse multiphoton ionization process in which intermediate states are shifted into resonance, it is not possible to see directly the effects of the temporal dependence of population transfer to the excited state. Since the intensity varies spatially for a focused beam, atoms in slightly different spatial locations will go through resonance at different times during the pulse. So all transition times are present for each pulse and the temporal effect is averaged. The fact that residual population has been observed for single-color experiments [9], however, shows that the excited states do act as storage states for population during the pulse. However, in short-pulse experiments (120 fs), the contribution to the ionization signal from rising-edge excitation may be minimal [10]. This lack of contribution may be due to the relatively fast rate at which the atoms pass through resonance with the excited states during the rising edge of the pulse. With the two-color, 100-ps-pulse experiment described here, it is clearly shown that the time at which the atoms make the transition to the excited state is an important factor in the photoionization probability because of the two-step process by which the total ionization occurs.

This work has been supported by the National Science Foundation.

[1] R. R. Freeman, P. H. Bucksbaum, H. Milchberg, S. Darack, D. Schumacher, and M. E. Geusic, Phys. Rev. Lett. **59**, 1092 (1987).
[2] O. L. Landen, M. D. Perry, and E. M. Campbell, Phys. Rev. Lett. **59**, 2558 (1987).
[3] T. J. McIlrath, R. R. Freeman, W. E. Cooke, and L. D. van Woerkom, Phys. Rev. A **40**, 2770 (1989).
[4] Shih-I Chu and J. Cooper, Phys. Rev. A **32**, 2769 (1985).
[5] R. M. Potvliege and Robin Shakeshaft, Phys. Rev. A **38**, 4597 (1988).
[6] Abraham Szoke, J. Phys. B **21**, L125 (1988).
[7] R. R. Freeman and P. H. Bucksbaum, J. Phys. B **24**, 325 (1991).
[8] M. Dorr, D. Feldmann, R. M. Potvliege, H. Rottke, R. Shakeshaft, K. H. Welge, and B. Wolff-Rottke, J. Phys. B **25**, L275 (1992).
[9] M. P. de Boer and H. G. Muller, Phys. Rev. Lett. **68**, 2747 (1992).
[10] G. N. Gibson, R. R. Freeman, and T. J. McIlrath, Phys. Rev. Lett. **69**, 1904 (1992).
[11] X. Tang, A. Lyras, and P. Lambropoulos, Phys. Rev. Lett. **63**, 972 (1989).
[12] H. P. Breuer, K. Dietz, and M. Holthaus, Z. Phys. D **10**, 13 (1988).
[13] J. G. Story, Ph.D. thesis, University of Southern California (1989).
[14] F. Gounand, J. Phys. (Paris) **40**, 457 (1979).
[15] C. E. Theodosiou, Phys. Rev. A **30**, 2881 (1984).